Available online at www.sciencedirect.com
ScienceDirect
Surface Science 600 (2006) 3141–3146
SURFACE SCIENCE
www.elsevier.com/locate/susc

Structural analysis of Si(1 1 1)–$\sqrt{21} \times \sqrt{21}$-Ag surface by reflection high-energy positron diffraction

Y. Fukaya [a,*], A. Kawasuso [a], A. Ichimiya [a,b]

[a] *Advanced Science Research Center, Japan Atomic Energy Agency, 1233 Watanuki, Takasaki, Gunma 370-1292, Japan*
[b] *Faculty of Science, Japan Women's University, 2-8-1 Mejirodai, Bunkyo-ku, Tokyo 112-8681, Japan*

Received 19 March 2006; accepted for publication 26 May 2006
Available online 16 June 2006

Abstract

The atomic structure of Si(1 1 1)–$\sqrt{21} \times \sqrt{21}$-Ag surface, which is formed by the adsorption of small amount of Ag atoms on the Si(1 1 1)–$\sqrt{3} \times \sqrt{3}$-Ag surface, was determined by using reflection high-energy positron diffraction. The rocking curve measured from the Si(1 1 1)–$\sqrt{21} \times \sqrt{21}$-Ag surface was analyzed by means of the intensity calculations based on the dynamical diffraction theory. The adatom height of the extra Ag atoms from the underlying Ag layer was determined to be 0.53 Å with a coverage of 0.14 ML, which corresponds to three atoms in the $\sqrt{21} \times \sqrt{21}$ unit cell. From the pattern analyses, the most appropriate adsorption sites of the extra Ag atoms were proposed.

Keywords: Surface structure; Reflection high-energy positron diffraction (RHEPD); Total reflection; Silicon; Silver

1. Introduction

In 1994, it has been found that a $\sqrt{21} \times \sqrt{21}$ super-lattice structure is induced by adsorption of Au adatoms on a Si(1 1 1)–$\sqrt{3} \times \sqrt{3}$-Ag surface [1,2]. Similar $\sqrt{21} \times \sqrt{21}$ periodicity was also observed by the adsorption of noble metal atoms such as Ag and Cu [3–5] and alkali metal atoms such as Na, K, and Cs [6–8]. The atomic configurations of the $\sqrt{21}$ structure family are considered to be the same because of similarity of the electronic structure. Furthermore, the $\sqrt{21} \times \sqrt{21}$-Ag surface shows a drastic increase in the electrical conductivity as compared to the Si(1 1 1)–$\sqrt{3} \times \sqrt{3}$-Ag surface [9]. Recently, the mappings of the Fermi surfaces have been performed to investigate the origin of the high electrical conductivity and make clear the mechanism of the doping with respect to the adsorption on the Si(1 1 1)–$\sqrt{3} \times \sqrt{3}$-Ag surface [10,11]. Because of importance as a prototypical two dimensional metal system, the adsorption on the Si(1 1 1)–$\sqrt{3} \times \sqrt{3}$-Ag surface attracts much attention. So far, the structure analyses were carried out by using the scanning tunneling microscopy (STM) [1,2,12] and surface X-ray diffraction (SXRD) [13]. However, the several kinds of structure models have been proposed and hence opinions are divided on this matter.

Nogami et al. proposed the structure model, where all the additional Au atoms sit on the center of Ag triangles of the original Si(1 1 1)–$\sqrt{3} \times \sqrt{3}$-Ag surface [1]. In Nogami's model, five Au atoms are included in the unit cell of the $\sqrt{21} \times \sqrt{21}$ super-lattice structure. Ichmiya et al. proposed that the Au atoms are situated at the center of the Si trimer [2]. The number of the Au atoms in Ichimiya's model is three. Tong et al. proposed another structure model, which resembles to the Nogami's model although the number of the additional atoms is four [12]. These models were built on the STM observations. Using the SXRD method, Tajiri et al. proposed the new model where the four Au atoms relatively aggregate to each other and one atom is apparent from them [13]. Tong et al. demonstrated that the honeycomb chained triangle (HCT) or

* Corresponding author. Tel.: +81 27 346 9330; fax: +81 27 346 9432.
E-mail address: fukaya.yuki99@jaea.go.jp (Y. Fukaya).

0039-6028/$ - see front matter © 2006 Elsevier B.V. All rights reserved.
doi:10.1016/j.susc.2006.05.045

inequivalent triangle (IET) structure of the original Si(1 1 1)–$\sqrt{3}\times\sqrt{3}$-Ag was preserved for the Si(1 1 1)–$\sqrt{21}\times\sqrt{21}$-Ag surface using the angle-resolved photoemission spectroscopy (ARPES) [14] and the core-level photoemission [15]. It should be noticed that the element of the adsorption atom is Ag for Tong model and is Au for the other models.

In this paper, we investigated the optimum adsorption site of the additional Ag atoms for the Si(1 1 1)–$\sqrt{21}\times\sqrt{21}$-Ag surface using the reflection high-energy positron diffraction (RHEPD). The RHEPD is a newly powerful tool to study the surface structure, especially, the topmost atomic positions [16,17]. The remarkable advantage using the RHEPD for the surface science study is that the total reflection occurs at the grazing incidence. In the total reflection region, the incident positron beam is not able to penetrate the bulk and hence the diffracted intensities include the information about only the topmost surface atoms. Analyzing the totally reflected intensities, we can accurately determine the atomic positions and the thermal vibrational amplitudes with respect to the topmost surface layer [18,19]. In this study, we measured the RHEPD rocking curves from the Si(1 1 1)–$\sqrt{21}\times\sqrt{21}$-Ag surface. From the intensity analysis based on the dynamical diffraction theory, we determined the optimum surface structure. To obtain the consensus, we also performed the RHEPD pattern analysis. We will show a new structure model suitable for the Si(1 1 1)–$\sqrt{21}\times\sqrt{21}$-Ag surface structure.

2. Experimental procedure

Samples with a dimension of $15\times5\times0.5\ \mathrm{mm}^3$ were cut from a *n*-type mirror-polished Si(1 1 1) wafer (resistivity: 1–10 Ω cm). These were flushed at 1470 K in 10 s a few times, followed by degassing at 600 K for several hours. After the cleaning, sharp 7×7 spots were confirmed by a reflection high-energy electron diffraction (RHEED). To produce a Si(1 1 1)–$\sqrt{3}\times\sqrt{3}$-Ag structure, one monolayer (ML) of Ag atoms were deposited on a Si(1 1 1)-7×7 surface kept at 770 K using a electron beam evaporator, where 1 ML corresponds to $7.83\times10^{14}\ \mathrm{cm}^{-2}$. Subsequently, the sample was cooled down to 110 K using liquid nitrogen. Additional deposition of Ag atoms was done on the Si(1 1 1)–$\sqrt{3}\times\sqrt{3}$-Ag surface at low temperature. The deposition was stopped when the $\sqrt{21}\times\sqrt{21}$ spot intensities by RHEED reached the maximum. The deposition amount was expected to be 0.14 ML from the evaporation rate.

The experiments were carried out in a ultra-high vacuum chamber equipped with a positron source of ^{22}Na and magnetic lens system [20]. The positron beam energy was set at 10 keV. In the measurement of rocking curves, the glancing angle (θ) was varied up to 5.9° at a step of 0.1° with the rotation of a sample holder. The RHEPD pattern was taken with a multi-channel plate and charge coupled device camera. The image of the pattern was installed in a personal computer. The temperature of the sample was measured using a thermocouple attached at the sample holder.

3. Results and discussion

Fig. 1(a) and (b) show the RHEPD patterns measured from the Si(1 1 1)–$\sqrt{3}\times\sqrt{3}$-Ag and Si(1 1 1)–$\sqrt{21}\times\sqrt{21}$-Ag surfaces, respectively. It should be noted that the RHEPD patterns displayed here are superposition of the left and right parts. When depositing the additional Ag atoms on the Si(1 1 1)–$\sqrt{3}\times\sqrt{3}$-Ag surface, the fractional-order spots accompanied with the Si(1 1 1)–$\sqrt{21}\times\sqrt{21}$-Ag surface appear in the higher order Laue zone. Especially, the (20/21 17/21) spots are clearly seen in the RHEPD pattern. Accordingly, the RHEPD intensities for the (1/3 1/3), (2/3 2/3) and their equivalent spots

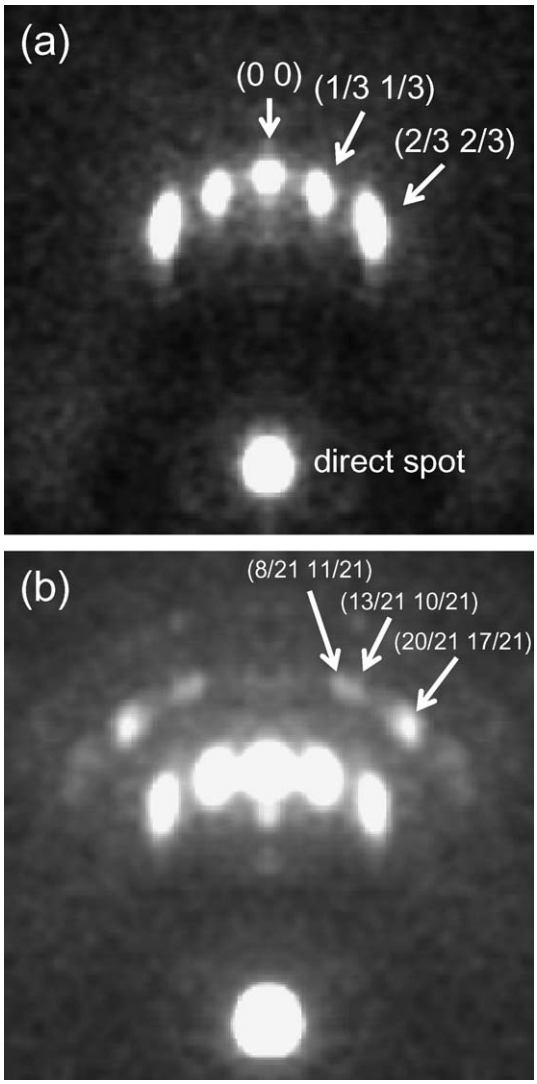

Fig. 1. RHEPD patterns observed from (a) the Si(1 1 1)–$\sqrt{3}\times\sqrt{3}$-Ag surface at $\theta=3.2°$ and (b) Si(1 1 1)–$\sqrt{21}\times\sqrt{21}$-Ag surface at $\theta=2.7°$. The incident azimuth corresponds to the [1 1 $\bar{2}$] direction. The substrate temperature is 110 K.

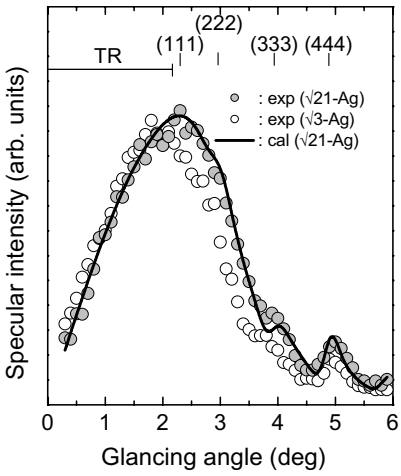

Fig. 2. RHEPD rocking curves for specular spots measured from the Si(1 1 1)–$\sqrt{3}\times\sqrt{3}$-Ag (open circles) and Si(1 1 1)–$\sqrt{21}\times\sqrt{21}$-Ag (closed circles) surfaces under the one-beam condition. Solid line shows the rocking curve calculated from the Si(1 1 1)–$\sqrt{21}\times\sqrt{21}$-Ag surface using the best-fit parameters of the additional Ag height and the coverage (see text). The positions of the Bragg reflections are labeled on the top of the figure. TR stands for the total reflection region.

decrease. In the RHEPD pattern, the formation of the $\sqrt{21}\times\sqrt{21}$-Ag structure is confirmed. The RHEPD pattern also shows the existence of the double domain of the $\sqrt{21}\times\sqrt{21}$-Ag structures, which correspond to the $\sqrt{21}\times\sqrt{21}(R\pm 10.89°)$ structures [12]. In the RHEPD pattern for the Si(1 1 1)–$\sqrt{21}\times\sqrt{21}$-Ag surface, the relative relation between the spot intensities I_{hk} is as follows; $I_{00} > I_{1/31/3} > I_{2/32/3} > I_{20/2117/21} > I_{8/2111/21} \sim I_{13/2110/21}$.

Fig. 2 shows the RHEPD rocking curves from the Si(1 1 1)–$\sqrt{3}\times\sqrt{3}$-Ag and Si(1 1 1)–$\sqrt{21}\times\sqrt{21}$-Ag surfaces, respectively. The incident azimuth is set at 7.5° away from the $[1\,1\,\bar{2}]$ direction, which is called one-beam condition [21]. Under the one-beam condition, the diffracted intensity can be expressed as a function of the layer spacing perpendicular to the surface and the atomic density in each layer because the simultaneous reflections parallel to the surface are sufficiently suppressed. As comparing with the rocking curve from the Si(1 1 1)–$\sqrt{3}\times\sqrt{3}$-Ag surface, the position of the intense and broad peak up to about 3.5° including the total reflection region shifts to higher angle for the Si(1 1 1)–$\sqrt{21}\times\sqrt{21}$-Ag surface. Here, the critical angle of the total reflection for the ideal Si(1 1 1) surface is estimated to be 2.0°.[1] However, the position of the (4 4 4) Bragg peak does not shift. Thus, owing to the adsorption of the additional Ag atoms, the crystal potential changes only at the topmost surface. It should be noted that the profile of the rocking curve in the total reflection region allow us to estimate the height of the adatoms before the detailed analysis [22]. When the adatom height is relatively high, a dip appears in the rocking curve in the total reflection region. The position of the dip obeys the Bragg equation [22]. For the Si(1 1 1)–$\sqrt{21}\times\sqrt{21}$-Ag surface, no apparent dip structure appears in the total reflection region. This means that the adatom height is considerably low. Thus, the additional Ag atoms are situated just above the underlying Ag layer. Since the crystal potential of the underlying Ag layer increases due to the superposition of the potential of the additional Ag atoms, the critical angle of the total reflection becomes high. Consequently, the position of the peak around the total reflection shifts to higher angle.

To determine the height of the additional Ag atoms precisely, we calculated the RHEPD intensities based on the dynamical diffraction theory [19,23]. The positions of the underlying Ag and Si layers were the same as the result of the first-principles calculations [24]. The mean squared amplitude of the thermal vibration for the Ag atoms was taken to be 8.90×10^{-2} Å at 140 K from the slope of the temperature dependence of the RHEPD intensities. The vibration amplitude for the Si atoms was determined to be 5.16×10^{-2} Å using the Debye-temperature of 610 K [25]. The absorption potential due to the electronic excitation for Si layers was fixed at 1.7 V [26]. As regards the Ag atoms, the absorption potential was assumed to be 0 V because the effect of the absorption in the topmost surface layer on the RHEPD intensity is sufficiently small [18,27].

Fig. 3 shows the rocking curves calculated from the Si(1 1 1)–$\sqrt{21}\times\sqrt{21}$-Ag surface with various heights of the additional Ag atoms. As mentioned above, under the one-beam condition, the shape of the rocking curve is very sensitive to the atomic positions normal to the surface. The calculated rocking curve drastically changes with the height (h_{ad}) of the additional Ag atoms. Up to $h_{ad} = 0.5$ Å, there are no significant changes in the shape of the rocking curve although the relative intensities are varied. Over $h_{ad} = 1.0$ Å, the distinct dip appears in the rocking curve, as denoted by arrowheads. The position of the dip gradually shifts to lower angle with increasing the height. In the measured curve, there is no distinct dip structure. Therefore, it can be ruled out that the height of the additional Ag atoms is higher than 1.0 Å.

To minimize the difference between the measured and calculated curves, the height of the additional Ag atoms was optimized. Considering the deposition rate for the preparation of the Si(1 1 1)–$\sqrt{3}\times\sqrt{3}$-Ag surface, the adsorption coverage of the additional Ag atoms corresponds to 0.14 ML (three atoms in the unit cell) for the Si(1 1 1)–$\sqrt{21}\times\sqrt{21}$-Ag surface. However, since actual adsorption amount of the additional Ag atoms was unknown, the coverage was varied as a parameter for the curve fitting. The goodness of fit was justified by a reliability (R) factor defined in Ref. [19]. As a result, it was found that after the optimization the height of the additional Ag atoms is 0.53 Å and the number of the additional Ag atoms is three (0.14 ML) in the $\sqrt{21}\times\sqrt{21}$ unit cell. The rocking

[1] The critical angle (θ_c) of the total reflection is calculated via Snell's equation as $\theta_c = \arcsin\left(\frac{V_0}{E}\right)^{\frac{1}{2}}$ [17], where E and V_0 are the accelerating voltage of the incident beam and the mean inner potential of the crystal, respectively. When $E = 10$ kV and $V_0 = 12$ V for the Si(1 1 1) surface, the value of θ_c is estimated to be 2.0°.

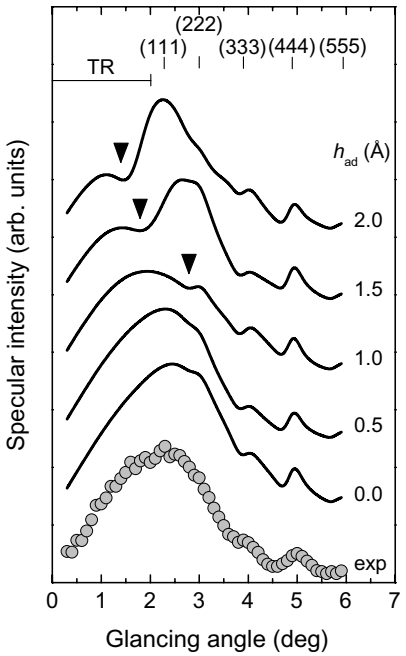

Fig. 3. Calculated RHEPD rocking curves for specular spots from the Si(1 1 1)–$\sqrt{21}\times\sqrt{21}$-Ag surface under the one-beam condition. The rocking curves denoted as solid lines were calculated with the heights (h_{ad}) of 0.0 Å, 0.5 Å, 1.0 Å, 1.5 Å, and 2.0 Å. These values indicate the heights of the additional Ag atoms from the underlying Ag layer. The coverage of the additional Ag atoms is set at 0.14 ML (three atoms in the unit cell). Closed circles represent the measured curve.

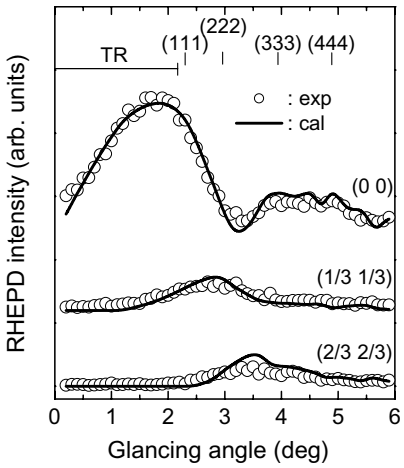

Fig. 4. RHEPD rocking curves for the (0 0), (1/3 1/3), and (2/3 2/3) spots from the Si(1 1 1)–$\sqrt{21}\times\sqrt{21}$-Ag surface along the [1 1 $\bar{2}$] direction. Open circles indicate the measured curves. Solid lines represent the rocking curves calculated using the best-fit model.

curve calculated using the optimum value is well in accordance with the measured one, as shown in Fig. 2. The adsorption coverage of 0.14 ML is supported by the core-level photoemission study [15]. The value of 0.53 Å is much smaller than that expected by means of the first-principles calculations [28]. The bond length between the additional Ag atom and the underlying Ag atoms will be discussed below.

To investigate the adsorption site of the additional Ag atoms in plane, we analyzed the RHEPD rocking curves at the symmetric azimuths. Fig. 4 shows the RHEPD rocking curves measured from the Si(1 1 1)–$\sqrt{21}\times\sqrt{21}$-Ag surface along the [1 1 $\bar{2}$] direction. The RHEPD calculations were achieved in a two-step process. First, the adsorption site for the additional Ag atoms was determined from the rocking curve analysis. Subsequently, the atomic configuration in the adsorption site was determined from the pattern analysis. In the rocking curve analysis, three different adsorption sites were considered: (i) center of the large Ag triangle in the IET structure, (ii) center of the small Ag triangle in the IET structure, and (iii) center of the Si trimer for the original Si(1 1 1)–$\sqrt{3}\times\sqrt{3}$-Ag surface. The number of the additional Ag atoms in the unit cell was taken at three, which was evaluated from the rocking curve analysis under the one-beam condition. The height of the additional Ag atoms from the underlying Ag layer was set to 0.53 Å. To identify only the adsorption site, we used the (0 0), (1/3 1/3), and (2/3 2/3) spots, the intensities of which are not sensitive to the atomic coordinates in each site.

Table 1 shows the value of R with various adsorption models having three additional Ag atoms in the unit cell. When the additional Ag atom is adsorbed on the center of the small Ag triangle or the Si trimer, the value of R becomes larger, i.e., the goodness of fit between the measured and calculated rocking curves becomes worse. It was found that all the additional Ag atoms sit on the center of the large Ag triangle of the IET structure. Aizawa and Tsukada demonstrated from the first-principles calculations that the surface structure having the Ag adatoms on the center of the large triangle is energetically stable by a factor of about 0.4 eV as compared with the other structures [28]. Therefore, our result is in consistent with the theoretical calculations with respect to the adsorption

Table 1
Reliability (R) factor for various structure models within three atom model

Structure model no.	1	2	3	4	5	6	7	8	9	10
Large Ag triangle	3	2	2	1	1	1	0	0	0	0
Small Ag triangle	0	0	1	2	1	0	1	2	3	0
Si trimer	0	1	0	0	1	2	2	1	0	3
R (%)	1.90	2.30	2.81	4.24	2.29	2.70	3.32	4.84	6.70	2.50

We calculated the R with changing the number of the additional Ag atoms on the centers of the large Ag triangle, small Ag triangle, and Si trimer for the IET structure of the Si(1 1 1)–$\sqrt{21}\times\sqrt{21}$-Ag surface.

site. Furthermore, we found that the value of R was improved when the surface structure was composed of the double domains of the $\sqrt{21}\times\sqrt{21}(R\pm 10.89°)$ structures. This is consistent with the result using the STM observations [14]. The rocking curves were also calculated when the underlying Ag structure was composed of the HCT configuration. As a result, we found that for the underlying Ag structure the IET structure is more plausible than the HCT structure. Thus, the IET structure of the original Si(1 1 1)–$\sqrt{3}\times\sqrt{3}$-Ag surface stable at low temperature is preserved even after the additional Ag deposition. The IET structure is sufficiently stable as the interface structure covered by the thin film remains the original structure [29]. Consequently, the rocking curve calculated using the structure model having three atoms on the centers of the large Ag triangles for the IET structure is in good agreement with the measured curve, as shown in Fig. 4.

From the rocking curve analyses, we found that the number of the additional Ag atoms is three and these are located on the center of the large Ag triangle with the height of 0.53 Å. However, the atomic configuration in the centers of the large Ag triangle is still unknown. Thus, we tried to verify the configuration by means of the pattern analysis. In particular, we focused on the intensity distribution lying on the 1/7th-Laue zone, which exists only in the case of the Si(1 1 1)–$\sqrt{21}\times\sqrt{21}$-Ag surface. The RHEPD patterns were calculated in a similar way of the rocking curve analysis. Fig. 5 shows the line scans of the 1/7th-Laue zone in the RHEPD pattern calculated using the three atom models. For the three atom model, five different structure models were considered, as shown in Fig. 6. Among these profiles, only the calculated pattern using the model 3 is well in accordance with the measurement. Therefore, from both the rocking curve and pattern analyses, it is concluded that the Si(1 1 1)–$\sqrt{21}\times\sqrt{21}$-Ag surface consists of the model 3. In this structure, the equilateral triangles composed of the addi-

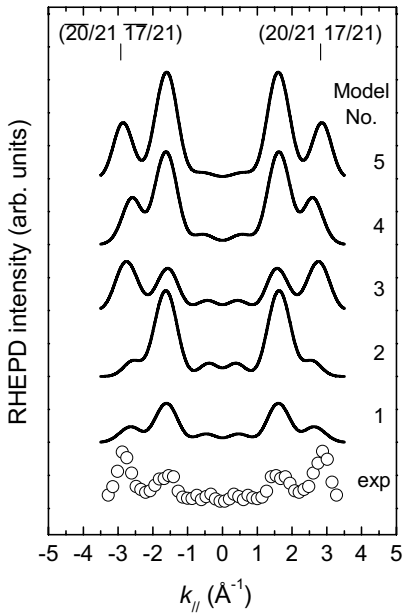

Fig. 5. Intensity distribution in the 1/7th-Laue zone of the RHEPD pattern from the Si(1 1 1)–$\sqrt{21}\times\sqrt{21}$-Ag surface as a function of wave number ($k_{\|}$) parallel to the surface. Open circles indicate the line profile extracted from the experimental pattern (Fig. 1(b)). The line profiles denoted as solid lines represent the calculated ones for the structure models, as shown in Fig. 6.

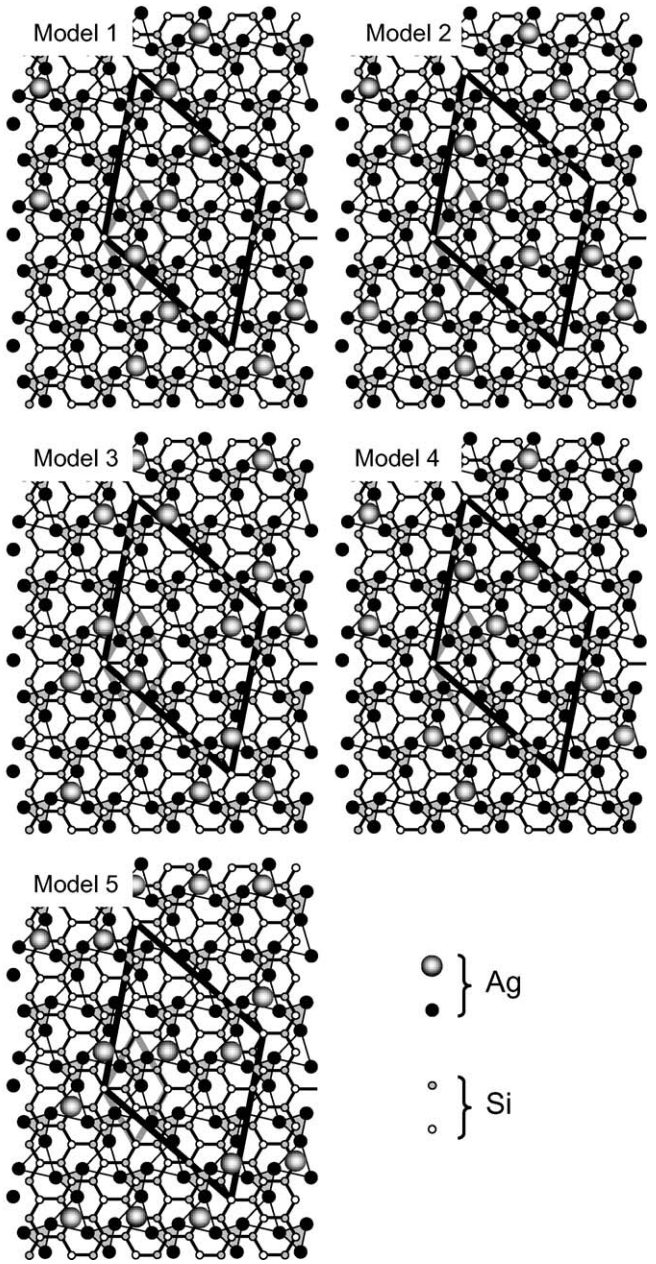

Fig. 6. Schematic drawings of the Si(1 1 1)–$\sqrt{21}\times\sqrt{21}$-Ag structure models for three atom model. Black and gray lines represent the unit cells of the $\sqrt{21}\times\sqrt{21}$ and $\sqrt{3}\times\sqrt{3}$ structures, respectively. Large and middle circles indicate the additional Ag atoms and the underlying Ag atoms, respectively. The other circles show the inner Si atoms. In these figures, the Si trimers are not displayed. The underling structure corresponds to the IET structure (denoted as large and small triangles) for the Si(1 1 1)–$\sqrt{3}\times\sqrt{3}$-Ag surface.

tional Ag atoms are located at the corners of the unit cell. This model is similar to the Ichimiya model with respect to the atomic arrangement of the additional atoms [2]. In model 3 of Fig. 6, the strain is most likely to become large at the center (small underlying Ag triangle) of the upper half unit cell. In the STM observations, the additional Ag atoms and the large strain parts might show brighter protrusions. In actual, the STM images observed in previous studies seem to reflect these features [1,2,12].

Finally, we consider the bond length between the additional Ag atom and the underlying Ag atom. From the rocking curve analysis, we found that the height of the additional Ag atoms is 0.53 Å. This value is much smaller than the theoretical calculation by about 1 Å. Since the spacing between the Ag atoms in the large triangle for the underlying IET structure is 3.94 Å [24], the bond length is determined to be 2.33 Å. As compared with the bond length (2.89 Å) between Ag atoms in the fcc crystal of the Ag bulk [30], the value of 2.33 Å is smaller by a factor of 20%. It has been reported by the ARPES studies that the charge transfer from the additional Ag atoms to the bulk takes place [14]. Since the atomic radius of the additional Ag atom is reduced due to the ionization, the bond length is considered to much shrink. The electrical conductivity for the Si(1 1 1)–$\sqrt{21}\times\sqrt{21}$-Ag surface is about four times as large as that for the Si(1 1 1)–$\sqrt{3}\times\sqrt{3}$-Ag surface [10]. When we consider the rigid band model for simplicity, the charge of 0.05 electrons per 1×1 unit cell is transferred into the substrate. The doping of electrons gives rise to short bond length of the additional Ag atoms.

4. Summary

In summary, we investigated the surface structure of the Si(1 1 1)–$\sqrt{21}\times\sqrt{21}$-Ag surface using the RHEPD. From the rocking curve analysis, we found that three additional Ag atoms in the unit cell are adsorbed on the center of the large Ag triangles of the original IET structure for the Si(1 1 1)–$\sqrt{3}\times\sqrt{3}$-Ag surface. The height of the additional Ag atoms from the underlying Ag layer is quite low (0.53 Å), which results from the ionization of the additional Ag atoms. It was found that in plane the equilateral triangles composed of the additional Ag atoms are arranged at the corners of the $\sqrt{21}\times\sqrt{21}$ unit cell. It is considered that the STM images obtained in the previous studies can be explained by this new model, e.g., by means of the first-principles calculations.

References

[1] J. Nogami, K.J. Wan, X.F. Lin, Surf. Sci. 306 (1994) 81.
[2] A. Ichimiya, H. Nomura, Y. Horio, T. Sato, T. Sueyoshi, M. Iwatsuki, Surf. Rev. Lett. 1 (1994) 1.
[3] Z.H. Zhang, S. Hasegawa, S. Ino, Phys. Rev. B 52 (1995) 10760.
[4] M. Lijadi, H. Iwashige, A. Ichimiya, Surf. Sci. 357–358 (1996) 51.
[5] S. Hasegawa, J. Phys. Condens. Matter 12 (2000) R463.
[6] C. Liu, I. Matsuda, H. Morikawa, H. Okino, T. Okuda, T. Kinoshita, S. Hasegawa, Jpn. J. Appl. Phys. 42 (2003) 1659.
[7] H.M. Zhang, K. Sakamoto, R.I.G. Uhrberg, Phys. Rev. B 70 (2004) 245301.
[8] M. D'angelo, M. Konishi, I. Matsuda, C. Liu, S. Hasegawa, T. Okuda, T. Kinoshita, Surf. Sci. 590 (2005) 162.
[9] for review, S. Hasegawa, X. Tong, S. Takeda, N. Sato, T. Nagao, Prog. Surf. Sci. 60 (1999) 89.
[10] I. Matsuda, T. Hirahara, M. Konishi, C. Liu, H. Morikawa, M. D'angelo, S. Hasegawa, Phys. Rev. B 71 (2005) 235315.
[11] J.N. Crain, M.C. Gallagher, J.L. McChesney, M. Bissen, F.J. Himpsel, Phys. Rev. B 72 (2005) 045312.
[12] X. Tong, Y. Sugiura, T. Nagao, T. Takami, S. Takeda, S. Ino, S. Hasegawa, Surf. Sci. 408 (1998) 146.
[13] H. Tajiri, K. Sumitani, W. Yashiro, S. Nakatani, T. Takahashi, K. Akimoto, H. Sugiyama, X. Zhang, H. Kawata, Surf. Sci. 493 (2001) 214.
[14] X. Tong, S. Ohuchi, N. Sato, T. Tanikawa, T. Nagao, I. Matsuda, Y. Aoyagi, S. Hasegawa, Phys. Rev. B 64 (2001) 205316.
[15] X. Tong, S. Ohuchi, T. Tanikawa, A. Harasawa, T. Okuda, Y. Aoyagi, T. Kinoshita, S. Hasegawa, Appl. Surf. Sci. 190 (2002) 121.
[16] A. Kawasuso, S. Okada, Phys. Rev. Lett. 81 (1998) 2695.
[17] A. Ichimiya, Solid State Phenom. 28&29 (1992/93) 143.
[18] A. Kawasuso, Y. Fukaya, K. Hayashi, M. Maekawa, S. Okada, A. Ichimiya, Phys. Rev. B 68 (2003) 241313(R).
[19] Y. Fukaya, A. Kawasuso, K. Hayashi, A. Ichimiya, Phys. Rev. B 70 (2004) 245422.
[20] A. Kawasuso, T. Ishimoto, M. Maekawa, Y. Fukaya, K. Hayashi, A. Ichimiya, Rev. Sci. Instrum. 75 (2004) 4585.
[21] A. Ichimiya, Surf. Sci. 192 (1987) L893.
[22] Y. Fukaya, A. Kawasuso, and A. Ichimiya, unpublished.
[23] A. Ichimiya, Jpn. J. Appl. Phys., Part 1 22 (1983) 176.
[24] H. Aizawa, M. Tsukada, N. Sato, S. Hasegawa, Surf. Sci. 429 (1999) L509.
[25] Y. Fukaya, A. Kawasuso, A. Ichimiya, e-J. Surf. Sci. Nanotech. 3 (2005) 228.
[26] G. Radi, Acta Crystallogr. 26 (1970) 41.
[27] Y. Fukaya, A. Kawasuso, K. Hayashi, A. Ichimiya, Appl. Surf. Sci. 244 (2005) 166.
[28] H. Aizawa, M. Tsukada, Phys. Rev. B 59 (1999) 10923.
[29] S. Horii, K. Akimoto, S. Ito, T. Emoto, A. Ichimiya, H. Tajiri, W. Yashiro, S. Nakatani, T. Takahashi, H. Sugiyama, X. Zhang, H. Kawata, Surf. Sci. 493 (2001) 194.
[30] C. Kittel, Introduction to Solid State Physics, John Wiley & Sons, 1997.